



Contents lists available at ScienceDirect

## Journal of Archaeological Science: Reports

journal homepage: [www.elsevier.com/locate/jasrep](http://www.elsevier.com/locate/jasrep)

## Palaeoenvironmental implications of a marine geoarchaeological survey conducted in the SW Argosaronic gulf, Greece

M. Geraga<sup>a</sup>, G. Papatheodorou<sup>a,\*</sup>, C. Agouridis<sup>b</sup>, H. Kaberi<sup>c</sup>, M. Iatrou<sup>a</sup>, D. Christodoulou<sup>a</sup>, E. Fakiris<sup>a</sup>, M. Prevenios<sup>a</sup>, S. Kordella<sup>a</sup>, G. Ferentinos<sup>a</sup>

<sup>a</sup> Laboratory of Marine Geology and Physical Oceanography, Department of Geology, University of Patras, 26 504, Greece

<sup>b</sup> Hellenic Institute of Marine Archaeology, 9, Saripolou Str., 106 82, Greece

<sup>c</sup> Hellenic Center for Marine Research (HCMR), Anavyssos, Greece

## ARTICLE INFO

## Article history:

Received 17 February 2016

Received in revised form 1 August 2016

Accepted 8 August 2016

Available online xxx

## Keywords:

Argosaronic gulf

Upper quaternary

Palaeogeography

Ancient shipwreck

Side scan sonar

Sub-bottom profiler

## ABSTRACT

A marine geoarchaeological survey was conducted at the southwestern end of the Argosaronic gulf in Greece, an area of archaeological importance. The survey was initiated by the discovery of a Late Bronze Age (LBA) shipwreck off Modi Islet. The survey which employed echo-sounding, sub-bottom profiling, side scan sonar systems and sediment coring extended to the area between Poros Island, Modi Islet and Argolid peninsula, aiming to evaluate the changes of the coastal zone extent in the past. The evolution of the palaeo-shoreline over the last 20 ka is proposed based on the interpretation of the acquired bathymetric and seismic records, the estimation of the thickness of the marine sediments and the examination of existing datasets of the relative sea level changes in the area.

The produced scenarios suggest that major changes marked the extent of the coastal zone since the Paleolithics. During the Upper Paleolithic period, the coast was larger by at least 11 km<sup>2</sup> and Poros and Modi islands were connected to the Peloponnesus. The sea level rise during the Mesolithic period formed a well-protected bay between Poros Island and Peloponnesus and disconnected the Modi Islet from Poros Island. The coastal zone reached the present configuration around Late Bronze Age. The detection and mapping of scarps on the seismic profiles imply that the sea level rise presented standstills at least from the Last Glacial maximum until the onset of Holocene. However, the submerged coasts could be potential areas of archaeological interest since the examined area is habitated continuously from the Paleolithic period.

The acoustic data sets produced high resolution geomorphological maps at the wreck site which constitute data base for the monitoring of the site. In addition, the examination of the seafloor texture at the wreck site suggests that the seafloor characteristics were unfavorable for the preservation of the shipwreck.

© 2016 The Authors. Published by Elsevier Ltd. This is an open access article under the CC BY-NC-ND license (<http://creativecommons.org/licenses/by-nc-nd/4.0/>).

### 1. Introduction

Archaeological investigations in the Argolid peninsula, located at the northeastern end of Peloponnesus, Greece (Fig. 1) have revealed rich archaeological findings which attest the human occupation of the area since the Paleolithic period. Among the onshore investigations of the area notable is the Franchthi cave located at the south Argolid peninsula (Fig. 1), presenting undoubted evidences for occupation since Upper Paleolithic period (Runnels and van Andel, 1987; Perles, 1987a & 1987b). In addition, the area includes permanent settlements of the Neolithic period in sites of the Argolid peninsula and numerous settlements since Early Helladic period in sites scattered in the Argolid peninsula and in the islands of Poros and Modi (Konsolaki-Giannopoulou, 2009; Tartaron et al., 2011). Offshore, surveying in this area has permitted to

discover two important ancient shipwrecks: the Dokos ancient shipwreck dated c. 2200 BCE (off Dokos Island, Papatheodorou et al., 1989–1992; Fig. 1) and the shipwreck of Point Irion (in the Argolid gulf) dated c. 1200 BCE (Lolos, 1999; Agouridis, 1999; Fig. 1) demonstrating that the southwestern part of the Argosaronic gulf was situated along in ancient navigation routes. In 2003, the Hellenic Institute of Marine Archaeology (HIMA; underwater survey directed by C. Agouridis) discovered off Modi Islet the remains of the cargo of a Late Bronze Age (13th–12th BCE) shipwreck (Agouridis, 2011). The age of the Modi shipwreck grants considerable archaeological value to the site since a few wrecks of the same age have been detected and studied in the eastern Mediterranean (i.e. at Capes Uluburum and Gelidonya, Bass, 1967, Pulak, 1998; along Carmel coast, Israel, Galili and Sharvit, 1999) providing evidence for seaborne trade in the region linked mostly to Crete and Cyprus (Wachsmann, 2011; Galili et al., 2013).

The recent research campaigns (in 2009, 2010 and 2013), on the Modi shipwreck incorporated, among others, marine geophysical

\* Corresponding author.

E-mail address: [gpathe@upatras.gr](mailto:gpathe@upatras.gr) (G. Papatheodorou).

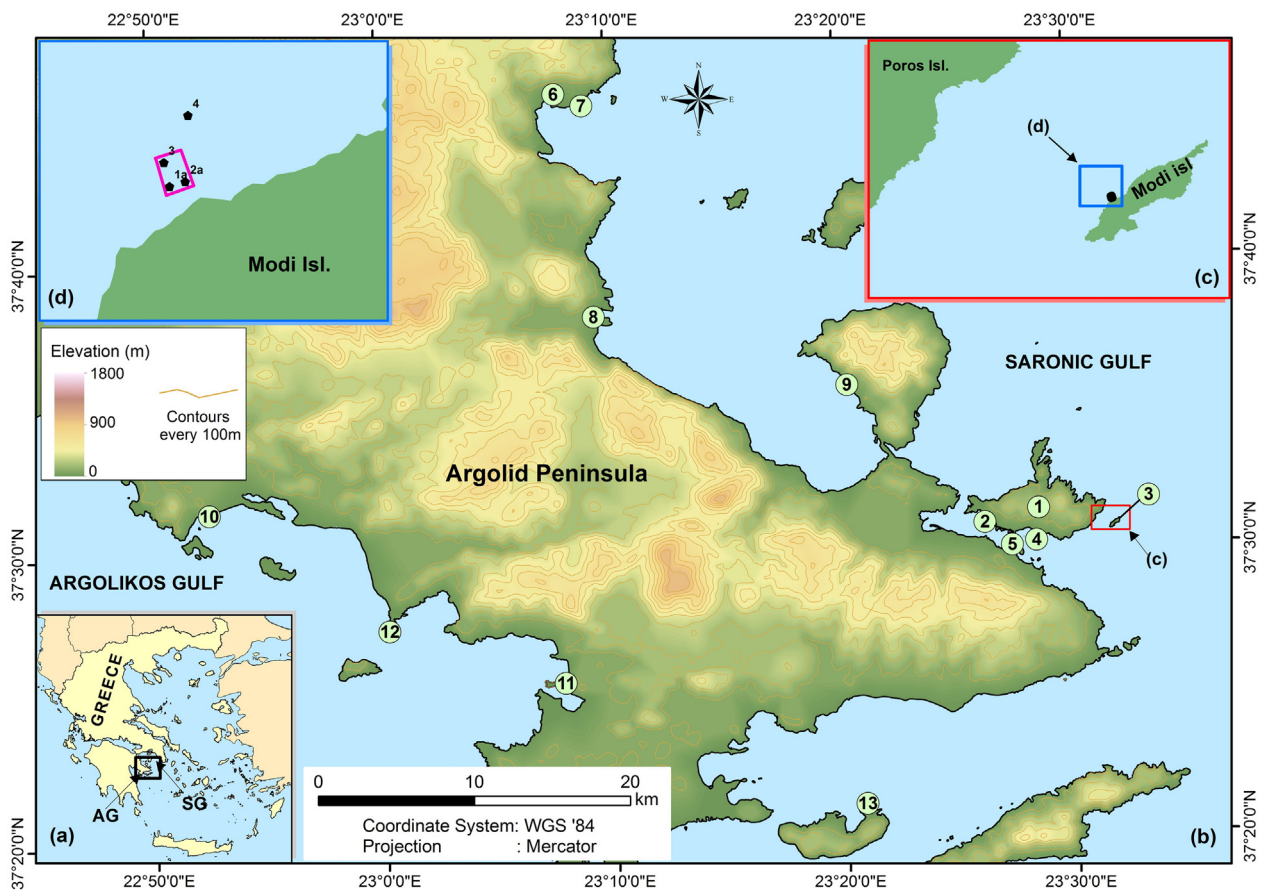


**Fig. 1.** Map of the studied area showing the location of the wreck and the core sites. The locations for sites discussed within text is also shown. (a) Map of Greece showing the Argolid peninsula and the location of Argolikos: AG and Saronic: SG gulfs. (b) Map of Argolid Peninsula presenting the location of: 1: Poros island (Kalauria), 2: Sfairia, 3: Modi island, 4: Monastiriou Bay, 5: channel between Poros and Argolid Peninsula, 6: Korphos bay, 7: Kalamianos bay, 8: Ancient Epidaurus, 9: Methana island (Vathi), 10: Tolo Bay, 11: Franchthi cave, 12: Point Irion shipwreck, 13: Dokos shipwreck. Red frame indicates the location of (c) inset. (c) Modi island presenting the location of the Late Bronze Age shipwreck. Blue frame indicates the location of (d) inset. (d) Detail map of the Modi shipwreck area presenting the location of the short sediment cores. Magenta frame indicates the area extending the ancient shipwreck. (For interpretation of the references to colour in this figure legend, the reader is referred to the web version of this article.)

surveying. The initial purpose of the marine geophysical surveying was the detailed acoustic mapping of the wreck site and the examination of the texture and stratigraphy of the seafloor, aiming to establish a data base capable of monitoring and assessing morphological change, natural and/or anthropogenic forcing, at the site (Quinn and Boland, 2010). However, the marine geophysical survey extended to a broader area between Poros Island, Modi Islet and Argolid peninsula aiming to detect features of potential archaeological interest and to evaluate the evolution of the coastal palaeogeography.

The sea level rise of the last glacial-interglacial cycle has caused major changes in coastal zones which have resulted the coastal landscapes and thus coastal prehistoric and historic settlements to submerge (Lambeck et al., 2002). The submerged coastal palaeo-landscapes constitute well preserved geo-archaeological records illuminating prehistoric and historic aspects of human life (Bailey, 2004, Bailey and Flemming, 2008) therefore there is a renewed interest for the detection, studying and in general, management of these sites in European level (e.g. SPLASCOS, n.d., SASMAP, n.d.). Fundamental practice for the surveying and studying of the unknown submerged archaeological sites is the establishment of a local geo-database combining datasets regarding the local geological, sedimentological and oceanographical processes and regimes aiming to evaluate the evolution of the palaeo-coastline (e.g. SPLASCOS, n.d., SASMAP, n.d.). The habitation from the Paleolithic era strengthens the interest in such investigation in the examined area. Furthermore, the examination of the evolution of the coastal palaeogeography in the examined area, it is expected to expand

prior knowledge gained by marine geophysical surveys conducted in the Argolid gulf (Van Andel and Lianos, 1984) and off Dokos Island (Papatheodorou et al., 2008) focused on the localization of the ancient coasts which marine transgression following the last glacial-interglacial cycle has inundated.

The marine geophysical survey in the present study comprised the acquisition and analysis of bathymetric, sub-bottom profiling and side scan sonar data. In underwater archaeological studies bathymetric data sets have been used for the examination of seafloor topography, the detection of possible surficial archaeological sites (e.g. Westley et al., 2011) and the monitoring of known archaeological sites (Quinn and Boland, 2010). Profiling surveying has been used to detect possible buried archaeological sites (e.g. Papatheodorou et al., 2005) and to evaluate the evolution of coastal palaeogeography (e.g. Chalari et al., 2009, Ferentinos et al., 2012, 2015). Side scan sonar data sets provides information for the seafloor texture and morphology and have been used for the detection and mapping of possible archaeological finds lying exposed on the seafloor (e.g. Quinn et al., 2007, Geraga et al., 2015). Furthermore sediment samples from short sediment cores collected from the area of the wreck were analyzed aiming to the determination of the sedimentation rate and the examination of the sedimentological characteristics of the seafloor at the wreck site. Although the employing of a varied acoustic datasets is a common practice in underwater archaeology, such surveys are rather limited in the Greek Seas and focus on the detection and mapping of ancient shipwreck (e.g. Sakellariou et al., 2007, Geraga et al., 2015) and coastal installation (e.g. Henderson et al., 2013, Ferentinos et al., 2015).

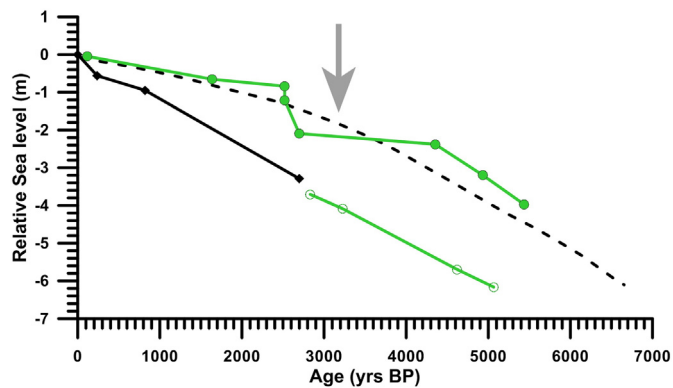


**Fig. 2.** Relative sea level change curves for the last 7 ka in the examined area. Dashed line: glacio-hydro-isostatic and eustatic corrected curve (Lambeck and Purcell, 2005), Black line: curve produced from geomorphological, historical and archaeological indications along the Peloponnesian coast of the Saronic Gulf and on the coast of Aegina and Poros islands (Kolaiti and Mourtzas, 2016), Green lines: curves based on data from sediments and beachrock formations from the northern part of Argolid peninsula (filled circles, Korphos bay, Nixon et al., 2009; open circles, Kalamianos bay, Dao, 2011). The arrow indicates the age of the shipwreck offshore Modi islet. The locations of the sites are shown in Fig. 1. (For interpretation of the references to colour in this figure legend, the reader is referred to the web version of this article.)

## 2. General geographical context

The study area is located at the southwestern end of the Saronic gulf (Fig. 1) and together with the area of the Methana Peninsula (northeastern side of Peloponnesus) comprise the upper western part of the

Hellenic Volcanic Arc. The wider region is characterized by volcanic and tectonic activity since the Pliocene/Pleistocene (Fytikas et al., 1986). Poros island is built of several different types of sedimentary, metamorphic and igneous rocks and Modi Islet includes mainly Cretaceous carbonates (Schwandner F.M., 1998).

Poros Island is separated from the northeastern Peloponnesus by a narrow channel which is up to 200 m wide. In the past, Poros consisted of two islands: Kalauria which was the larger one and Sfairia which was located at the south (Fig. 1). Pausanias noted that there was a strait between the two islands at the 2nd century A. D. (Pausanias, *Description of Greece*, 1961, Book 2: Corinth, Chapter 33). Through time the marine passage between the two islands was covered by debris and an isthmus developed connecting the two islands to one: the island of Poros.

Climatic, isostatic and tectonic factors have been resulted to significant changes of the coastal geography of the examined area. Models incorporating predictions for eustatic and isostatic changes of the sea level change point out that the sea level rose up to 130 m since the last 20K yrs and up to 6 m over the last 6K yrs (Lambeck and Purcell, 2005). However, underwater archaeological data found at sites around the Argolid peninsula (Methana, Epidauros, Tolo, Flemming et al., 1971; Porto-Heli, Pavlopoulos et al., 2012), data from sediments and beachrock formations from the northern part of Argolid peninsula (Korphos bay, Nixon et al., 2009; Kalamianos bay, Dao, 2011) and data from geomorphological, historical and archaeological indications along the Peloponnesian coast of the Saronic Gulf and on the coast of Aegina and Poros islands (Kolaiti and Mourtzas, 2016) suggest that the total area is under subsidence at least during the Holocene (Fig. 2). Based on previous studies, the estimations of the subsidence rate ranges between 1.0 and 1.5 mm/yr (Flemming, 1978), between 0.6 and

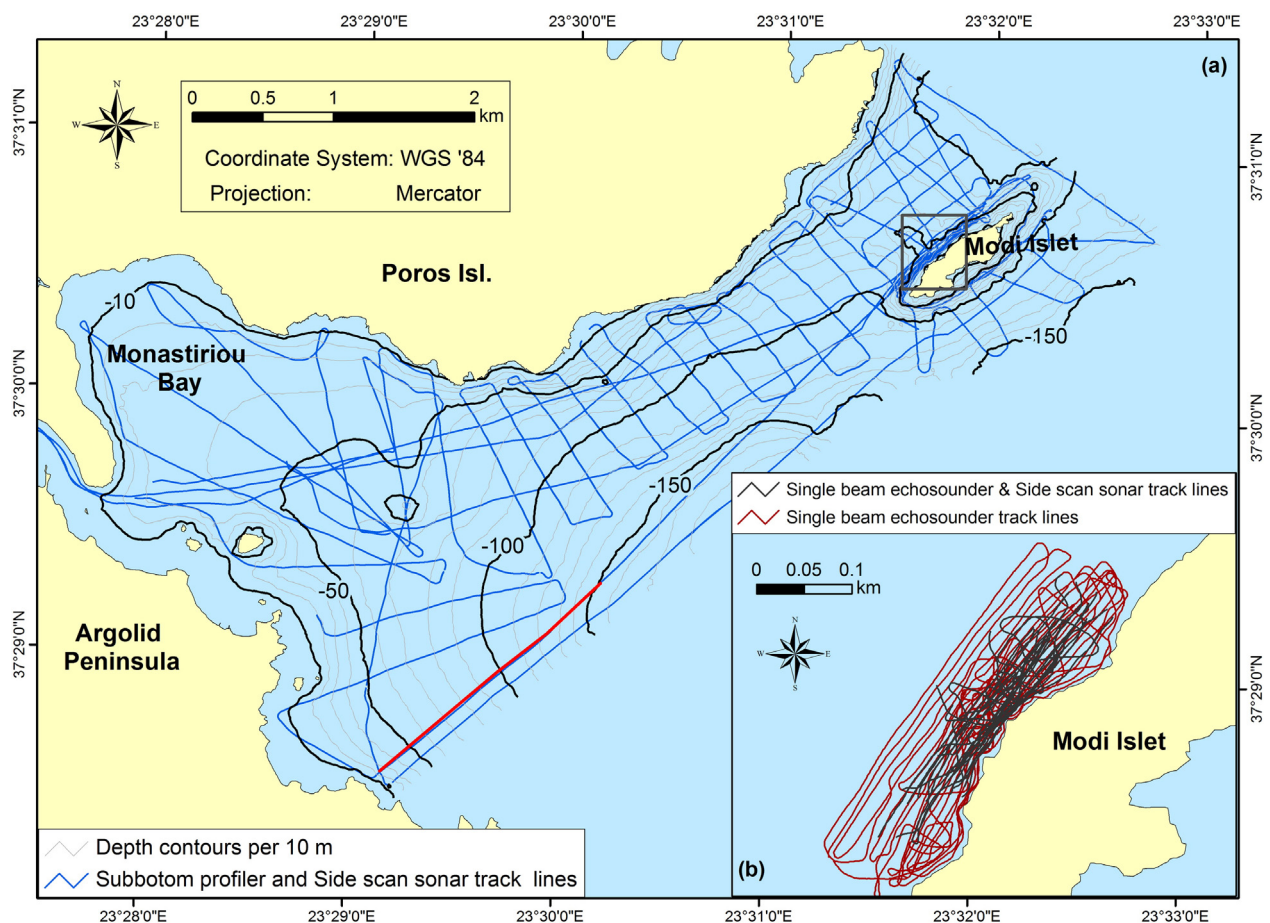


**Fig. 3.** (a) Map showing the tracklines for the sub-bottom profiler and side scan sonar in the examined area. Red line marks the location of the seismic profile presented in Fig. 5. (b) Detail map of the North coast of Modi Island showing the single beam echosounder and side scan sonar track lines above the area of the ancient shipwreck. (For interpretation of the references to colour in this figure legend, the reader is referred to the web version of this article.)

1.3 mm/yr (Lambeck, 1995) and between 0.3 and 0.7 mm/yr (Pavlopoulos et al., 2012). Furthermore, the datasets from Korphos bay (Nixon et al., 2009) and along the western coast of the Saronic Gulf (Kolaiti and Mourtzas, 2016) suggest that the sea level rise was not gradual but conducted in jumps related to tectonic activity though the absolute age of the sea level stands is not similar between the studies.

### 3. Archaeological settings and submarine findings

Modi Islet is located 1.06 km southeast from the ancient Kalauria Island (Fig. 1). The location and probably the shape and the coastal morphology of the island turned it an important landmark to ancient navigation routes and to a trading post of the Aegean Sea (Agouridis, 1997, 2011). The discovery of an impressive settlement of the Late Bronze Age period verified the archaeological importance of the small rocky island (Konsolaki-Giannopoulou, 2009). The settlement which is dated at the 13th century BCE flourished for 100 to 150 years and then vanished suddenly probably due to fire as an ash layer has been detected all over the remnants (Konsolaki-Giannopoulou, 2009). However, the importance of the study area in the trade of Aegean region and in particular that of olive oil and wine since the Proto–Helladic period is also verified by the cargoes of the two ancient shipwrecks: the Dokos and Point Irion shipwrecks (Fig. 1; Papathanasopoulos et al., 1989–1992; Agouridis, 1999; Lolos, 1999).

The cargo of the Modi shipwreck consists of pottery assemblage scattered on the north rocky slopes of the islet at a water depth between 25 and 38 m (Fig. 1; Agouridis, 2011). The pottery assemblage which has been located and recorded to date comprises jars, pithoi and hydrias which, together with other pottery fragments such as bases, rims and handles, raise the number of the large transport vessels from the ship's cargo to the number of at least 45 items, all dated to the Late Bronze Age

(13th–12th c. BC) and comparable in types with other shipwreck cargoes and trading centers of the Aegean of the same period. (Agouridis, 2011). Previous underwater archaeological research has been focused on the mapping of the site by photogrammetric techniques and the documentation of the findings. The marine geophysical survey on the site focused on the mapping of the site by acoustic techniques aiming to the reconstruction of a detailed geomorphological map of the area combining data sets for the seafloor texture and stratigraphy.

### 4. Materials and methods

#### 4.1. Marine geophysical techniques

The present study employed (i) an echo-sounder for the acquisition of bathymetric data sets and the examination of the seafloor topography in particular at the wreck site, (ii) a side scan sonar for the examination of the seafloor texture, the detection of possible targets of archaeological importance and the mapping of the site of the ancient wreck and (iii) a sub-bottom profiler for the determination of the seafloor stratigraphy, the detection of possible buried targets of archaeological importance and the comparison with side scan sonar data for the rejection of possible targets as natural (i.e. rocky outcrops).

The present study utilized (i) an Elac Nautic Hydrostat 4300 digital single-beam hydrographic echosounder capable of accuracy of less than 5 cm in shallow water environments, (ii) a side scan sonar system consisting of an 272TD dual frequency (100 and 500 kHz) towfish and an Edgetech 4100P topside digital recording unit and (iii) a 3,5 kHz sub-bottom profiling system consisting of a Model 5430A GeoPulse Transmitter, a Model 5210A GeoPulse Receiver, a Triton Imaging Inc. digital acquisition and recording unit and an O.R.E. Model 132B over-the-side four transducers array. The positioning and navigation conducted with a Hemisphere V100 D.G.P.S. capable of accuracy less than

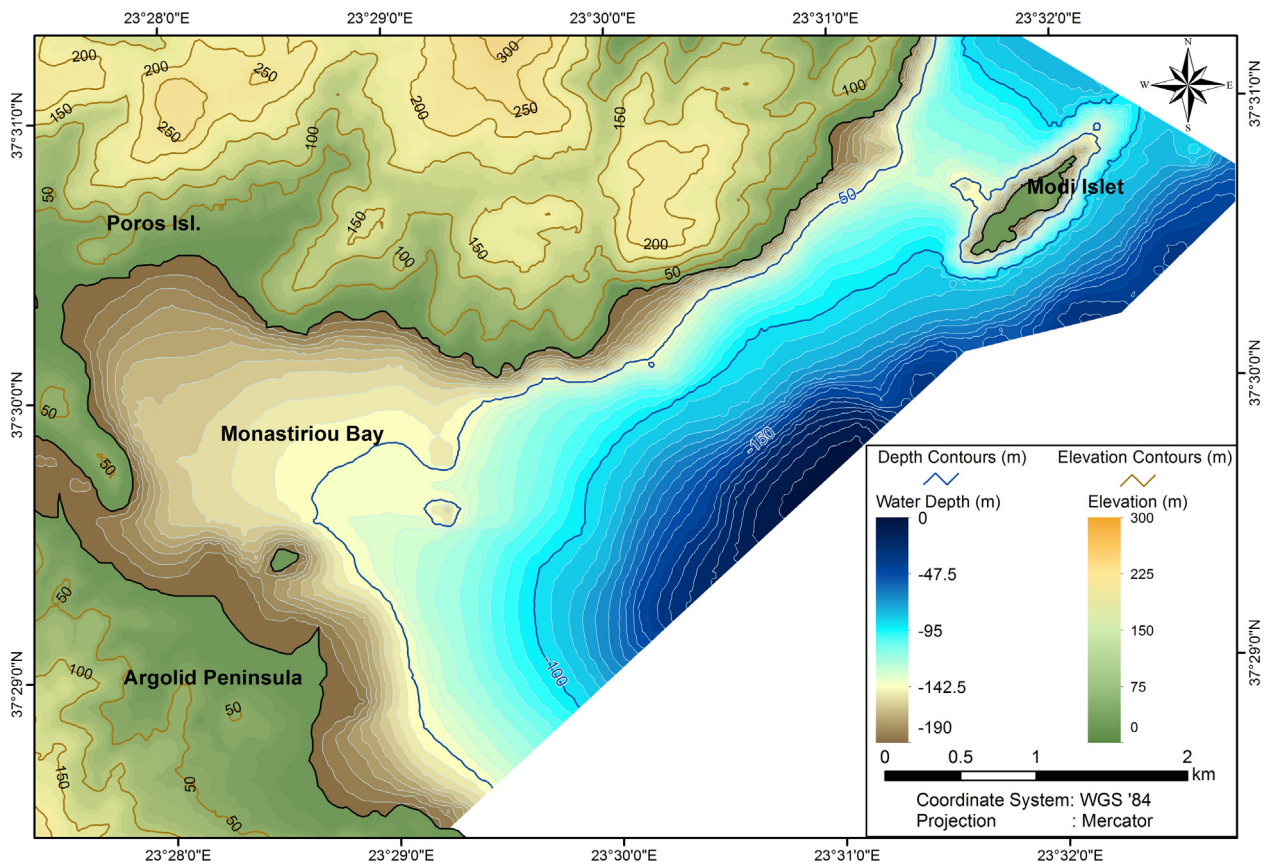


Fig. 4. Bathymetric map of the survey area.

1.5 m. All instruments were connected to the navigation and positioning system enabling the georeferencing of all the acquired datasets. The survey was conducted on board the vessel “Agios Nikolaos” RCh 290 (provided by H.I.M.A.), which was modified to meet the specifications of the remote sensing survey.

Bathymetric data acquired from a grid of tracklines 151.5 km in total length (Fig. 3). The grid was denser at the site of the wreck. An area of about 14 km<sup>2</sup> was insonified by the side scan sonar system (Fig. 3). During the surveying the lane spacing provided a 50% range overlap. The towfish height above the seafloor ranged between 10 and 50% of the slant range. The operational frequency was 100 kHz when the surveying was focused on the detection and mapping of the seafloor texture and morphology and 500 kHz when it was focused on the mapping of areas of interest such as the wreck site. Sub-bottom profiling conducted upon a grid with the majority of the tracklines running vertical to the coastline examining the coastal palaeogeography and detection of palaeoshoreline features (Fig. 3). A total length of 135 km of 3.5 kHz sub-bottom profiles were acquired using a time base of 0.1 s and a 0.1 ms pulse length providing a vertical resolution less than 0.5 m.

Side scan sonar data were processed using ISIS Sonar (Triton Imaging Inc.) software and then were mosaiced at 0.5 m resolution using DelphMap (Triton Imaging Inc.) software. In the present survey, high backscatter, which is attributed to hard substrate, is presented by light tones on sonographs. Low backscatter (soft substrate) is presented by dark tones and acoustic shadow by black tone. The processing of the profiles was undertaken by the SB-Interpreter (Triton Imaging Inc.) software. For the interpretation of the seismic stratigraphy the determination of the Echo Types was based on the variation of the sharpness, continuation frequency and the amplitude of the recorded seismic (acoustic) reflectors (Damuth, 1975). All the processed datasets were compared and synthesized in GIS.

## 4.2. Coring

Four short cores (M1a, M2a, M3a and M4) of undisturbed sediments were retrieved by SCUBA divers by hand using a Kajak corer at water depths ranging between 27 and 36.4 m. (Fig. 1). The maximum depth of core penetration was 30 cm. The cores were sealed and stored at low temperature. Sediment samples from two of these cores (M3a and M4) were collected for the estimation of sedimentation rate, grain size analyses and analyses of benthic foraminifera composition. The core M3a is located within the area of the wreck site and the other (M4) out of it.

## 4.3. Sediment analyses

The actual sediment accumulation rates was estimated at two sites (M3a and M4) using the <sup>210</sup>Pb method. This method has been used as stand-alone technique (i.e. Naeher et al., 2012) or in combination with other dating methods for the age estimation of marine sediments (Noble et al., 2016). In the present study this method has been used for the determination of the sedimentation rate. The downcore <sup>210</sup>Pb activity was determined by  $\alpha$ -counting of its grand-daughter, <sup>210</sup>Po, assuming secular equilibrium with <sup>210</sup>Pb. The method published by Sanchez-Cabeza et al. (1998) was employed for the total dissolution of sediments. Briefly, dried sediments were digested successively with HNO<sub>3</sub>-HClO<sub>4</sub>, HF and HCl. Polonium-210 isotopes were deposited on silver discs and counted on a total alpha counter (Ortec EG & G). Below the 5 cm sediment layer in core M3a the <sup>210</sup>Pb activities were almost constant; thus the average value of these activities was assumed as the supported <sup>210</sup>Pb activity. The same value was used for core M4. The mean apparent sedimentation rate was calculated following the constant rate of supply (CRS) model of Appleby and Oldfield (1978). For core M3a, the sampling interval was 1 cm I until 5 cm depth and then every 10 cm until the 30 cm depth layer. For core M4, the intervals

varied from 3 to 1 cm down to 6.4 cm. The analyses conducted at the Hellenic Center for Marine Research (HCMR) laboratories.

The grain size and micropaleontological analyses conducted in the Laboratory of Marine Geology and Physical Oceanography, Department of Geology, University of Patras. These analyses conducted for the examination of the texture of the sedimentary deposits at the area of the wreck and the surround seafloor. The macroscopic observation of the two cores suggested that both consist of homogenous coarse-grained material. The sediment samples collected with a sampling interval ranging between 5 and 10 cm in each core, covering all the length of the core.

For the determination of the grain size parameters of the sediment samples, dry sieving method and a Malvern Mastersizer 2000 Hydro were used.

Micropalaeontological analysis was conducted on the same sediment samples, following the standard methods (i.e. Geraga et al., 2010; Naeher et al., 2012): the samples were disintegrated by hydrogen peroxide and were then sieved with mesh widths of 63, 150 and 500  $\mu$ m. So far the fraction sediment between 150 and 500  $\mu$ m has been microscopically examined. The dry and weighed samples were split into separate aliquots. At least 300 foraminifera specimens were identified following the generic classification of Loeblich and Tappan (1987). Each taxon was expressed as a percentage of the total assemblage.

## 5. Results

### 5.1. Bathymetry

The water depth of the examined area is up to 190 m (Fig. 4). In the western most part of the surveyed area, the seafloor is smooth and

**Table 1**

Synthetic representation of the Acoustic Types (AT), Echo Types (ET) and Acoustic Backscatter Patterns (ABP) detected in the examined area.

Acoustic Type (AT)	Echo Type (ET)	Acoustic Backscatter Pattern (ABP)	Interpretation (ground-truthing)
1	ET1	ABP4a	Rocky seafloor
2	ET2a	ABP1	Seafloor covered by thick sedimentary cover
3	ET2b	ABP2	Rocky seafloor close to surface with no outcropping
4	ET2d	ABP3	<i>Posidonia oceanica</i> meadows
5	ET2c	ABP4b	Coralligene formations
6	ET1	ABP4c	Targets

deepens gently seawards forming a wide shelf of around 2 km in width up to 50 m water depth. This pattern is disturbed only seawards Monastiriou bay, where local appearances of rocky outcrops elevating the seafloor for about 20 m (from 55 m to 35 m water depth). At the eastern part of the surveyed area and around the Modi Islet the seafloor is steeper with slopes ranging between 26° and 37°. Furthermore, a topographic high connects Modi Islet to Poros Island. This ridge like formation is up to 65 m deep and has 35 m maximum water depth towards Modi Islet and 32 m towards Poros Island.

### 5.2. Echo types and seismic stratigraphy

The sea-bottom in the acquired records is characterized by two different Echo Types (ET 1–2) (Table 1). ET 1 is characterized by a surface reflector without any evidence of a deeper signal penetration. This reflector appears sharp and continuous but locally accompanies surface hyperbolae; echoes of weak and strong amplitude with low to high vertex elevation above the seafloor.

ET 2 is characterized by a continuous surface reflector overlying an acoustically transparent unit. The base of the transparent unit is recorded as a prolonged, continuous and in general flat reflector which prevented further acoustic penetration representing the acoustic basement. The acoustic signature of the surface reflector, together with that of the transparent unit distinguishes ET 2 type into four subtypes. In ET 2a the transparent unit is well developed and it has a thickness

between 1.5 and 4 m. Locally weak internal reflectors of less than the amplitude of the seafloor reflection are present. The transparent unit in ET 2b though clearly recognized less than 1.5 m thick. ET 2c accompanies a surface reflector with hyperbolae echoes of weak amplitude with low vertex elevation above the seafloor and a weak acoustic basement. In ET 2d the surface reflector appears semi-prolonged and discontinuous with a less transparent unit underneath and a very weak acoustic basement.

ET 1 dominates the steep slopes of the Modi Islet and inclined up to 38° the north and up to 35° southwards developing to a point easily recognized on the bathymetry. ET 1 corresponds to the acoustic basement of Modi Islet.

Furthermore, the detailed examination of the seismic profiles acquired in the present study show the presence of numerous scarps detected at several depths on the surface of the acoustic basement (Fig. 5). These features flat surface breaks and rises steeply. The majority of them appear buried under thin sedimentary deposits. Similar features have been obtained on the seismic records acquired from the shelves of the Argolid gulf (Van Andel and Lianos, 1984) and of Dokos Island (Papatheodorou et al., 2008) and they have been attributed to submerged shore markers (palaeoshorelines) where the base of each feature corresponds approximately to past sea level stands.

In the present study the depths of 189 scarps cluster in specific levels (Fig. 5b). The most frequent observed depths of the scarps obtained at around 32–36 m, 46–48 m, 50 m, 56–58 m, 66–68 m, 80–90 m, 95 m,

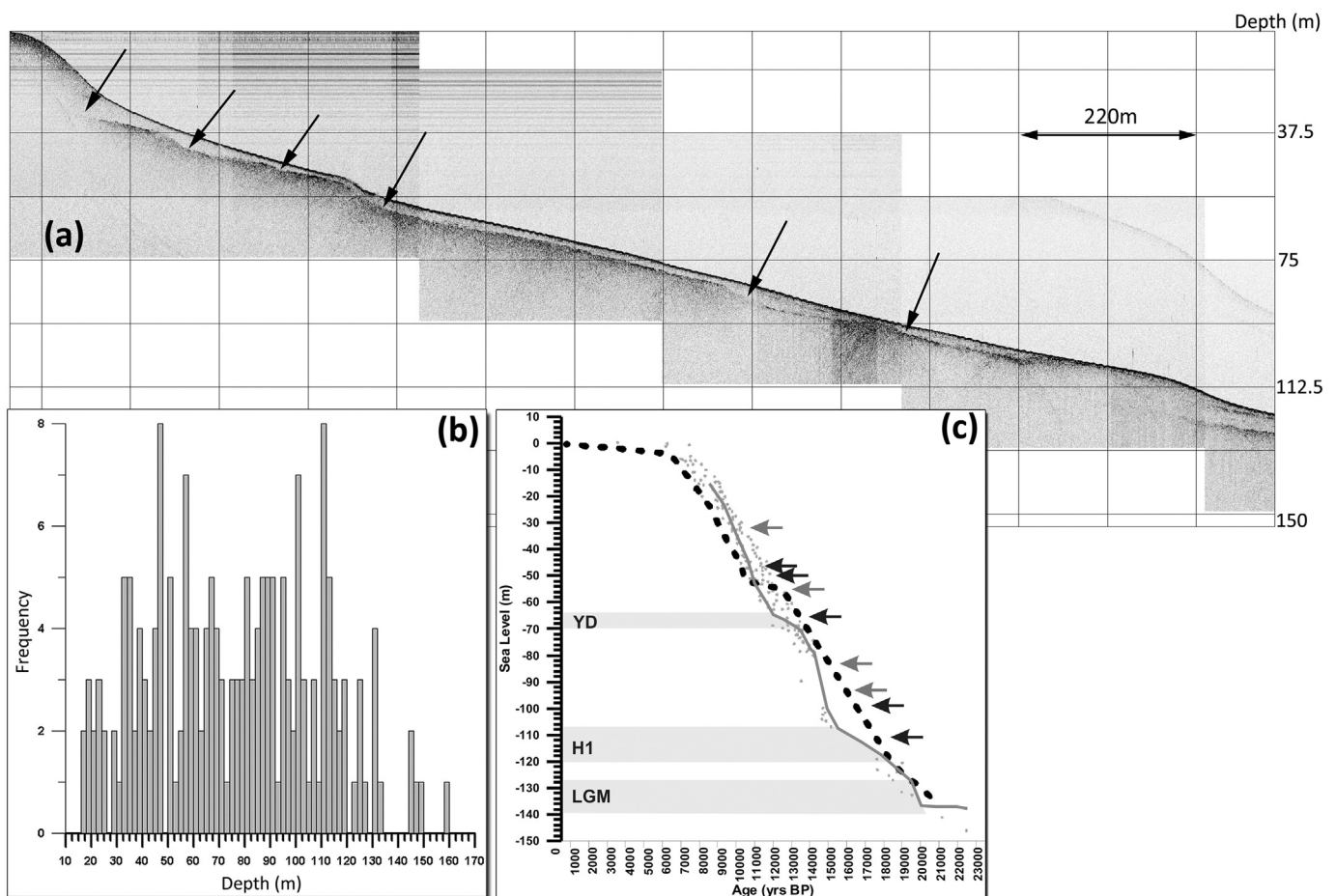


**Fig. 5.** (a) Seismic profile showing the presence of the palaeo-shore features (scarps). (b) Histogram of submerged scarps obtained on seismic reflection records, plotted against depth below present sea level. (c) Diagram showing the water depth of the most frequent clusters of scarps (arrows) on sea level change curves. The dashed line presents the sea level change of Argolid peninsula (Lambeck, 1996, Lambeck and Purcell, 2005). The grey points show the global sea level change (Lambeck et al., 2002) and the grey line a generalized global sea level change curve based on the latter data (Yokoyama and Esat, 2011). Grey zones indicate the coldest intervals of the last 20 ka (YD: Younger Dryas, H1: Heinrich 1, LGM: Last Glacial Maximum; Yokoyama and Esat, 2011). Black arrows indicate the clusters of groups which have been also obtained from the shelves of the Argolid gulf (Van Andel and Lianos, 1984) and of Dokos Island (Papatheodorou et al., 2008). The location of the profile is shown in Fig. 3.

100 m and 110–114 m. The occurrence of the scarps in specific levels may suggest temporal sea level standstills due to climatic and/or tectonic events. The clusters of depths were compiled to the sea level change curve for the area (Argolid peninsula, Lambeck, 1996) and to the global sea level curve (Lambeck et al., 2002, Yokoyama and Esat, 2011) in an attempt to evaluate the age of their formation (Fig. 5c). The comparison showed that the clusters most probably correspond to ages ranging between 18 and 9 kyrs BP. This time span corresponds to the transition from the Last Glacial Maximum to early Holocene and it includes short term climatic oscillations. Although the age estimations are not very confident it is noticeable that four (4) of them coincide with temporal steps of the sea level evolution obtained on the local and/or the global sea level curves. The two group of depths at 100 m and 110–114 m, dated around 17 kyrs BP coincide in age with the prevalence Heinrich 1 (H 1) event and the two group of depths at 57 m and 67 m coincide in age with the prevalence of the Younger Dryas event.

### 5.3. Side scan sonar imagery

Distinctive tonal patterns revealed from the 100 kHz mosaic (Fig. 6) include four Acoustic Backscatter Patterns (ABP 1–4) (Table 1). ABP 1 includes wide areas of dark and homogenous backscatter but ABP 2 displays wide areas of medium reflectivity. ABP 3 characterizes areas of high backscatter with striped often alternating between light and dark tones. The boundary of the pattern is distinct and often interlaced. ABP 4 includes areas of high reflectivity with a patchy tonal character. This pattern was further distinguished into three types (ABP 4 a to c) based on the acoustic signature on the sonographs. ABP 4a usually is accompanied on sonographs by areas of acoustic shadow. ABP 4b shows a “spotted reflectivity” and in most cases accompanied by a clear

acoustic shadow on the far, side due to the elevation of the central area. Ring-like zones of high backscatter encircle the base of the central area. ABP 4c includes small areas of high reflectivity with more or less certain shape (geometry) accompanied with narrow zones of acoustic shadow.

### 5.4. Sediments

Fig. 7 presents the results of the analysis conducted on the sediment samples from the examined short sediment cores M3a and M4. Based on the grain size analysis the sediment cores (M3a and M4) consist of gravely sand and slightly gravely sand without any sedimentary layers. The mean size ranging between 554 and 594  $\mu\text{m}$  (Folk, 1974). In addition, similar foraminiferal assemblages obtained in all examined samples (Fig. 7). In all sediment samples the proportion of benthic to planktonic is high. The dominant benthic genera are *Amphistegina*, *Peneroplis*, *Quinqueloculina*, *Asteriginata*, *Elphidium*, *Cibicides*, *Rosalina*, *Discorbis*, *Planorbulina* and *Textularia*. These benthic assemblages are typical for shallow seafloor of the Aegean Sea covered probably by seagrass (Koukousioura et al., 2011). Therefore the micropaleontological analysis suggests a shallow marine origin for the examined sedimentary interval.

The  $^{210}\text{Pb}$  analyses suggest an average sedimentation rate for the two cores of 0.05 cm/yr (Fig. 8). This finding is comparable with the sedimentation rate estimated for the nearshore zone of the Northern Argolid peninsula from previous studies ranging between 0.06 and 0.05 cm/yr (based on estimations from the Table 2, provided by Nixon et al. (2009)). Low sedimentation rate (0.01 cm/yr) has been also estimated for the Myrtoon basin located south of the surveying area (Geraga et al., 2000).

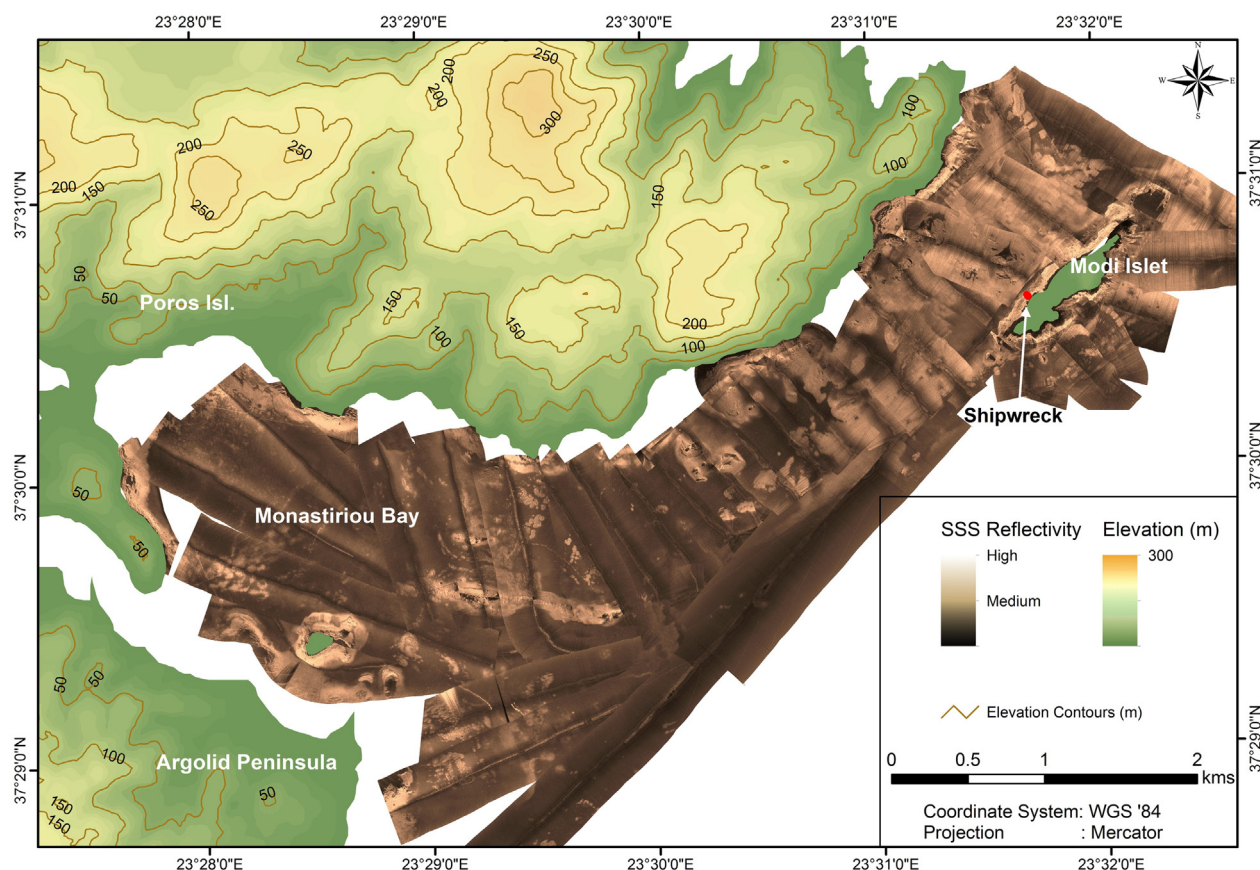
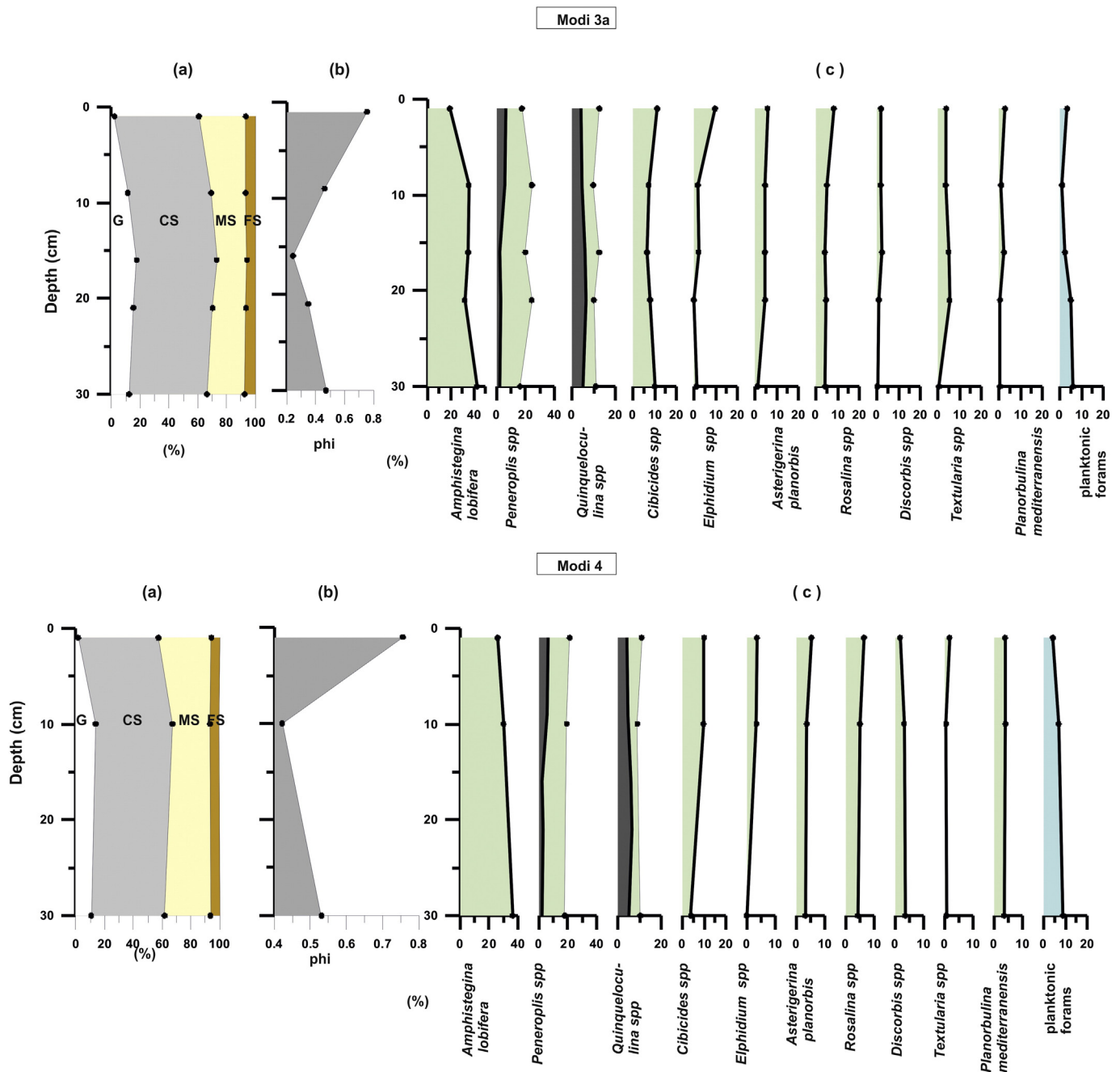


Fig. 6. Side scan sonar mosaic (100 kHz) retrieved from the examined area. Geographic Coordinate system: WGS 1984, Mercator projection.



**Fig. 7.** Down core variation of the data from the sediment analysis for the short sediment cores Modi 3a (up) and Modi 4 (down). (a) Distribution of grain size, G: Gravel, CS: Coarse Sand, MS: Medium Sand, FS: Fine Sand, (b) mean grain size in phi and (c) the benthic foraminifera composition. The grey bands indicate the participation of *Peneroplis planatus* and *Quinqueloculina berthelotiana* within the relative diagrams.

## 6. Discussion

### 6.1. Synthesis of the acoustic data

The comparison and the synthesis of the seismic profiling and side scan sonar data distinguish five Acoustic Types (AT 1–5; see Table 1) in the examined seafloor. Each AT incorporates specific Echo Types (ET) and Acoustic Backscatter Patterns (ABP) thus comprising specific seismic stratigraphy and seafloor substrates, respectively. Fig. 9 presents the spatial distribution of these ATs in the surveyed area. AT 1 comprise ET 1 and ABP 4a and corresponds to rocky seafloor. This type was mostly recorded in shallow waters, close to the coastline and locally in deeper waters forming small areas around bathymetric shoals. The AT 1 has been recorded peripheral to the Modi Islet and it includes also the wreck site.

This texture of the seafloor probably provoked the preservation of the shipwreck. It is likely that the rocks caused strong damages at the wooden hull during the wrecking event, spilling the content on the seafloor and leaving behind a debris field exposed to corrosion and biological processes of deterioration in open seawater (Wheeler, 2002, Wachsmann, 2011). The coarse grained sediments which also have high bearing capacities and in addition high oxygen penetration are unfavorable for the preservation of the shipwreck remains (Gregory, 2006).

AT 2 comprises ET 2a and ABP 1 and corresponds to a seafloor covered by thick sedimentary cover. AT 2 is the dominant seabed type in the examined area (Fig. 9). The presence of internal reflectors depicts variations in the sedimentary deposits due to changes in grain size, density or water content. AT 3 comprises ET 2b and ABP 2 and corresponds



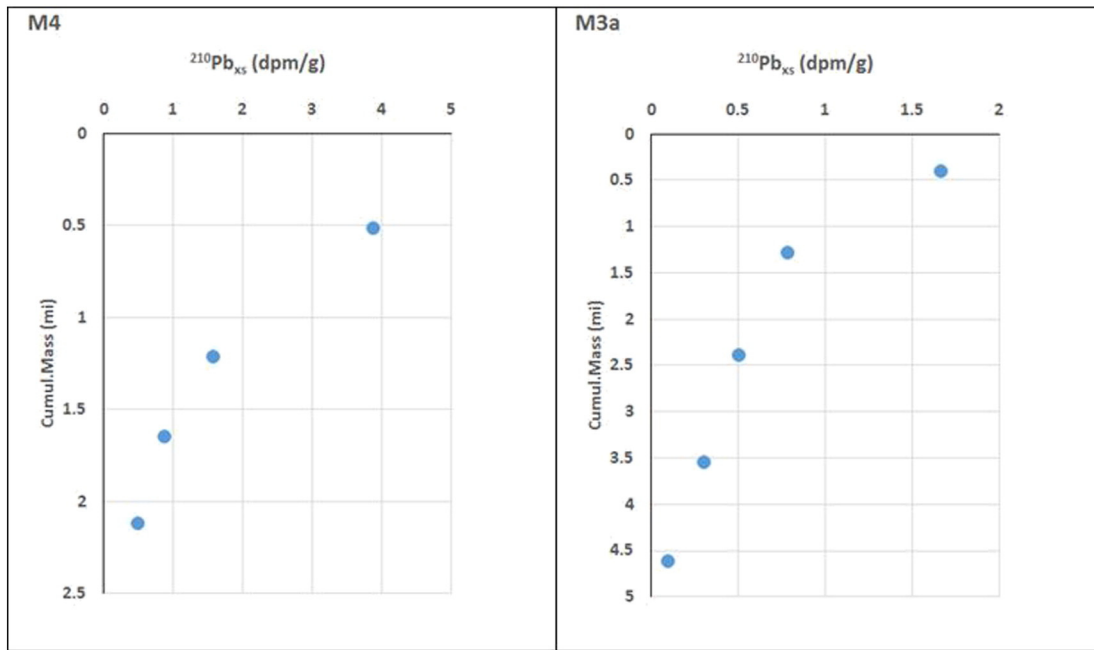


Fig. 8. Vertical profiles of <sup>210</sup>Pb excess versus cumulative mass for short sedimentary core M4 (left) and M3a (right).

to a seabed where the rocky basement shallows but without outcropping the seafloor. Upon the rocky seafloor a thin veneer of loose sediments has been deposited. AT 3 has been recorded only in the eastern part of the examined area and seems to run close to the AT 1 (Fig. 9). The thickness of the upper, almost transparent unit of ET 2 was estimated and mapped regardless of the acoustic signature that it presents between the subtypes. Fig. 10 presents the spatial distribution of the thickness of the sedimentary cover in all examined areas. Based on this map, in the eastern part of the surveyed area the accumulation of the sediment is higher and appears to increase gradually seawards forming in a small basin.

AT 4 comprises ET 2d and ABP 3 represents a seafloor covered by dense distributed seagrass probably of *Posidonia oceanica*. The gas-filled channels within the seagrass plants, along with gas bubbles produced during photosynthesis are the dominant causes for the strong backscatter surrounding the seagrass meadows on the sonographs (Kiparissis et al., 2011). This type is observed in the shallow waters of the western part of the examined area (Fig. 9). AT 5 comprises ET 2c and ABP 4b and detected locally to form small areas scattered in the eastern part of the examined area and in the western part between the isobaths of 70 and 130 m. This type corresponds to a seafloor where coralligène formations have been built up. These benthic organisms form colonies, like

small reefs, by hard, usually calcified, casings producing localized strong backscatter facies and hyperbolic echoes on seismic profiles (Georgiadis et al., 2009). Due to their nature, the acoustic signature of these biogenic reefs on side scan sonar and profiling records can be misinterpreted as rocky formations if the reefs are developed on hard substrates; or as artificial sites (i.e. remains of wrecks) if the reefs are developed on soft substrates (i.e. remains of wrecks) if the reefs are developed on soft substrates (Geraga et al., 2015). Both the above marine habitats (*Posidonia oceanica* and coralligène formations) are under the protection of the EU (European Union Habitats Directive - Annex I, Dir 92/43/CEE for *P. oceanica* and, European Commission, 2006 for coralligène formations.). Both these habitats constitute significant fisheries. In the present study linear and almost parallel alternations of high and low backscatter detected on sonographs around coralligène formations are attributed to trawling marks and confirm the intense fishery activity on the area.

6.2. Detection of artifacts

The side scan sonar imagery signature of the seafloor at the wreck site corresponds to ABP 4 and locally to ABP 2, suggesting the dominance of rocky seafloor covered at preferred sites by a thin veneer of loose sediments of coarse grain sized (Section 5.4). Rocks occur together

Table 2

Estimation scenarios for the palaeodepth (Pd) at specific periods, using the equation Pd = D – Psl – Tsub + Sth (Ferentinis et al., 2012). The palaeo-sea level (Psl) is from the data of Lambeck, 1996 and Lambeck and Purcell, 2005; Fig. 5c). The seafloor subsidence (Tsub and thus the Psl + Tsub component) is given for three cases (0.0007 m/yr, Pavlopoulos et al., 2012; 0.001 m/yr, Flemming, 1978, Lambeck, 1995 and 0.0015 m/yr, Lambeck, 1995). The sediment thickness (Sth) presents the maximum value added. This component was initial applied to the sediment thickness map (Fig. 10) (to ensure the addition of this component only at those points of the map where the sedimentary deposits are thicker than that of the calculation) and then to the final maps. In the present work the maps calculated with a subsidence rate of 0.0007 m/yr and a sedimentation rate of 0.005 cm/yr (grey columns) are presented and discussed.

Archaeological period	Age (yrs BP)	Psl (m)	Tsub (m/yr)			Psl+Tsub (m)			Sth (m)
			(a) 0.0007	(b) 0.001	(c) 0.0015	(a)	(b)	(c)	
Upper Paleolithic	20000	130	14	20	30	144	150	160	10
Mesolithic	9000	30	6.3	9	13.5	36.3	39	43.5	4.5
Neolithic	7000	10	4.9	7	10.5	14.9	17	20.5	3.5
Late Bronze Age	3265	2	2.2855	3.3	4.9	4.3	5.3	6.9	1.6

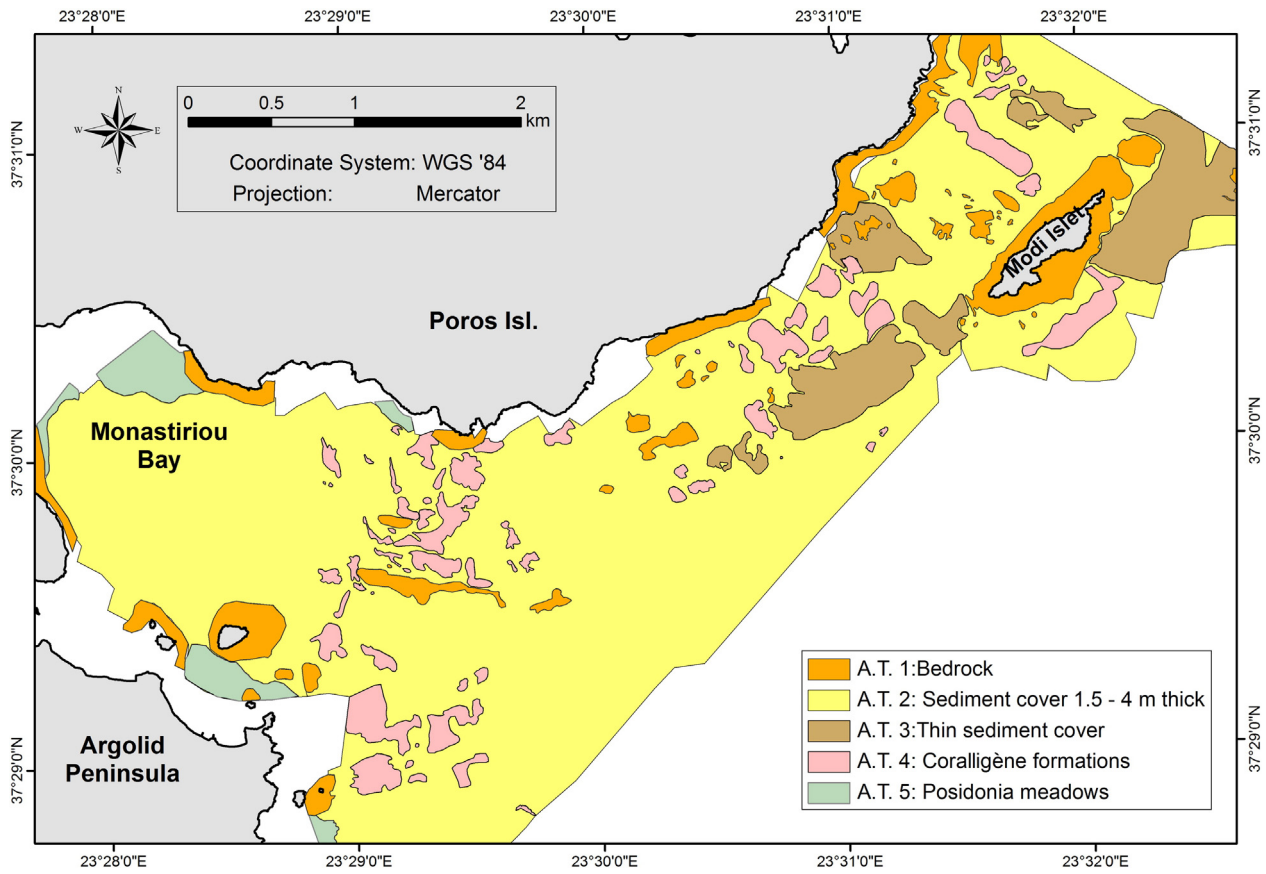


Fig. 9. Morphological submarine (seafloor) map retrieved after combining the seismic stratigraphy and the seafloor backscatter patterns in the survey area.

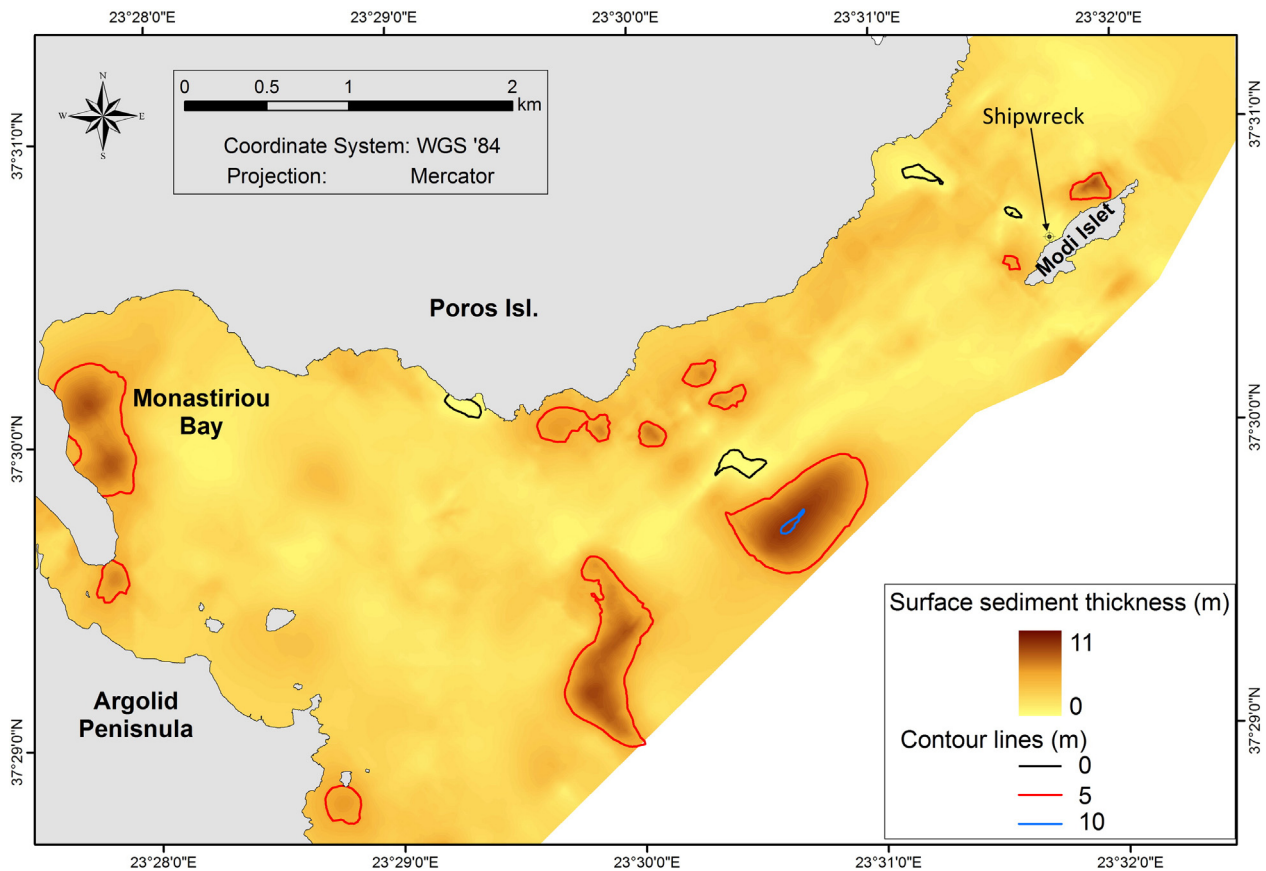
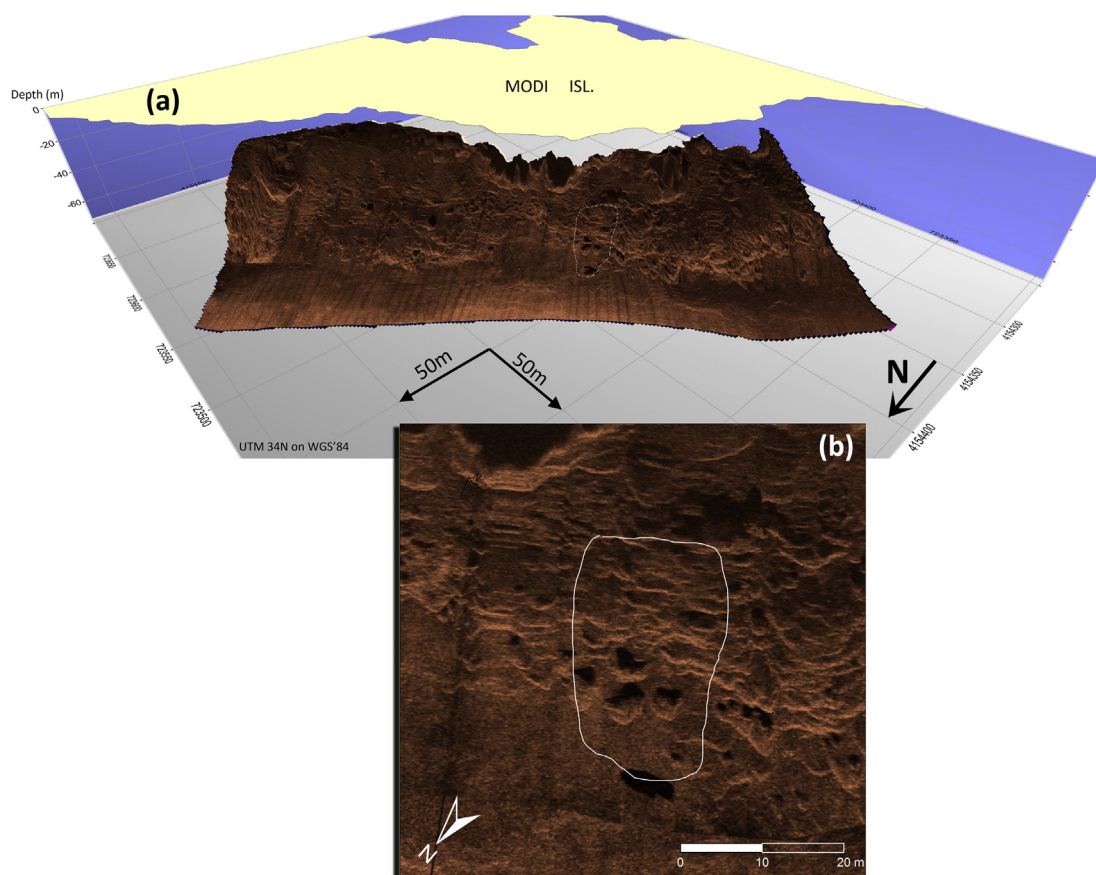


Fig. 10. Map showing the spatial distribution of the sedimentary deposits (thickness of the upper unit of echo type 2 (ET 2)) as obtained from the seismic profiles from the survey area.



**Fig. 11.** (a) 3-D georeferenced map produced after the compilation of high resolution sonographs (500 kHz) and the bathymetric data, at the area of wreck site showing by the dashed white line (b) Detail map of the area of the Modi shipwreck.

with the remains of the cargo consisting of whole and fragmentary artifacts scattered on the seafloor (Agouridis, 2011), providing patchy backscatter records of high to medium intensity. This backscatter pattern corresponds to the uneven topography of the site formed by mixture of irregular rocks and ceramics. On this seafloor where the distances between the ceramics and the rocks were very short ranging between few and zero centimeters and the sizes of the artifacts whether they appear as intact or as fragments were always lower than the topographic highs of the rocky seafloor, the detection of the archaeological artifacts by acoustic means was not attainable.

Anyway, the area of the wreck site wasinsonified by high resolution frequency (500 kHz) and in combination with the high resolution bathymetric and profiling data sets, a detailed geomorphological map of the area was produced. This map is expected to establish a robust geo data base for the monitoring of the site and the evaluation of possible accretion – erosion morphological changes (Quinn and Boland, 2010). Fig. 11 presents a 3D-like georeferenced image from the area of the wreck site produced by the synthesis of the side scan sonar mosaic and the bathymetric dataset.

Beyond the wreck site, the detection of potential archaeological sites in the examined area also proved more complex than it was expected mostly due to the presence of the coralligène formation. As mentioned before, in the examined area the coralligène formation appears often as minute reefs of small extent (10 × 20 m) and height (1–5 m) of which their sonographs show strong backscatter facies providing an inaccurate indication for potential sites of interest. However, the comparison of the side scan records with those of the seismic profiles added more criteria for their identification and thus improved the classification of natural sites and sites of potential interest. Eight (8) sites evaluated as more promising. The acoustic signature of these sites usually

corresponds to ABP 4c on the side scan sonar recordings. At least in one case the ground truthing survey by drop camera verified a site as the remains of an aircraft of the World War II (Fig. 12). The ground truthing for the rest of the sites is an ongoing survey.

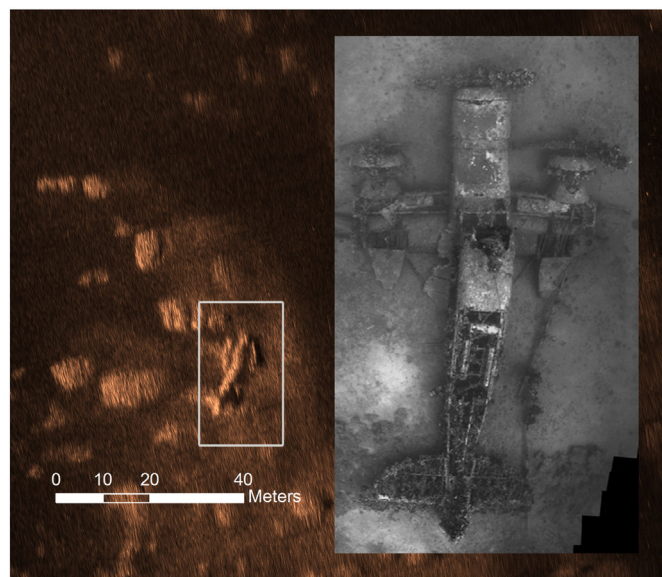


**Fig. 12.** Side scan sonar mosaic and underwater photo from towing camera verifying the remains of an aircraft (WWII; Photo credit: Vasilis Mentogiannis). For ethical and legal reasons the exact location (coordinates) of the site is not given.

### 6.3. Implications for the shoreline evolution

In the examined area, coastal palaeogeography reveals significant changes since the Late Paleolithic time. Interactive geodynamic processes, linked to the continental and to marine environment or human activities, of global or regional scale are the driven factors influencing these changes. However, among them, the climatic change associated with the last glacial-interglacial cycle seems to be the dominant factor causing eustatic and hydro glacio isostatic changes of the sea level. The rise of sea level after the end of Last Glacial period caused the inundation of large coastal areas and the submergence of possible coastal archaeological installations. The evaluation of the ancient coastal evolution appears crucial in the surveying for the location and detection of potential underwater archaeological sites.

In the present study, efforts were made to evaluate the location of the coastline in specific periods based on the above; together with the datasets obtained from the seismic profiles and the marine sedimentation rate in the wreck site. For that, we used the equation proposed by Ferentinos et al. (2012),  $Pd = D - Psl - Tsub + Sth$ , where: Pd is the palaeo-depth at a specific period, D is the present day depth, Psl is the palaeo-sea level at a specific period, Tsub is the total seafloor subsidence and Sth is the thickness of the accumulated sediment over the same period (Table 2). Fig. 13 presents the location of the coastline at the Upper Paleolithic (~20 kyrs), Mesolithic (~9.5 kyrs), Neolithic (~7 kyrs) and the Late Bronze Age (at the time of the wrecking). For these predictions we used the sea level curve as this has been constructed from the effect of the eustatic and isostatic factors in the area (Lambeck, 1996;

Lambeck and Purcell, 2005), an average subsidence rate of 0.7 mm/yr (Pavlopoulos et al., 2012) and a mean sedimentation rate of 0.05 cm/yr as this revealed from the marine sediments of the present study. According to the above estimations the sea level was stood 155 m below present sea level during Paleolithic, 40 m during Mesolithic, 18 m during Neolithic and around 6 m during the Late Bronze Age, at the time of the wreck.

Based on these prediction maps the rise of the sea level has caused important changes in coastal geography in the examined area (Fig. 13). The low sea level during the Paleolithic times had exposed large areas of the present seafloor configuring a broad coastal zone of smooth slopes (Fig. 13a). At those times the islands of Poros and Modi were connected and both islands constituted part of the present Argolid peninsula.

During Mesolithic, the previous coasts had been inundated (Fig. 13b). A large part of the ridge that develops between Modi and Poros islands was underwater and only a small part was exposed providing a step-stone configuration between the two islands. Furthermore a series of exposed reefs were developing a natural protected cove at the southwestern Poros island at the current location of Monastiriou Bay (Fig. 13b). The sea level stand in Neolithic times had turned the configuration of the coastal zone in forms similar to present day (Fig. 13c). Then Modi Islet was completely disconnected to Poros Island and the previous cove had now flooded (Fig. 13c). During the Late Bronze Age, at the time of the wrecking event, relative sea level was very close to present day similar to the coastal configuration seen today (Fig. 13d).

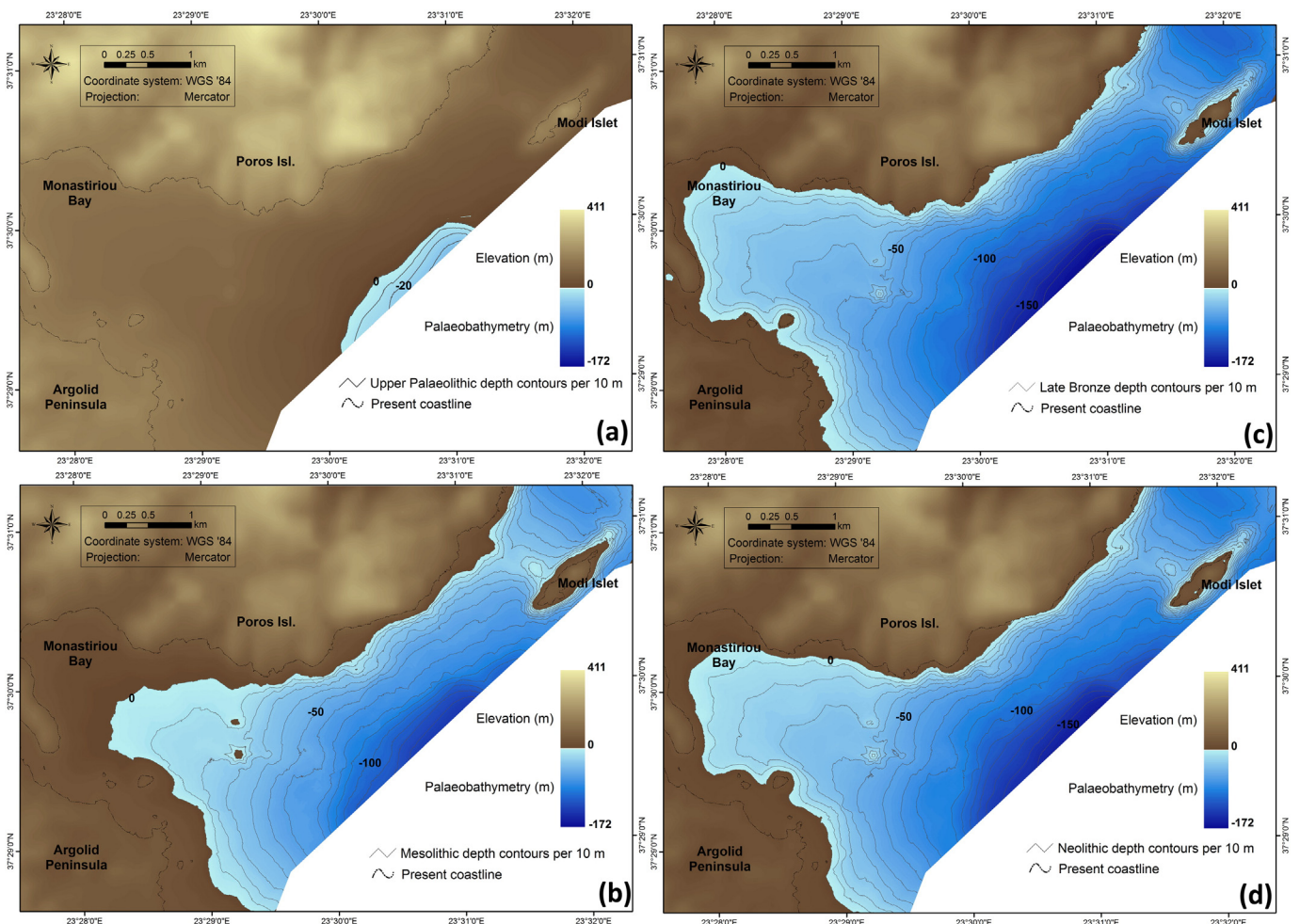


Fig. 13. Prediction maps for the coastal zone of: (a) Paleolithic period, (b) Mesolithic period, (c) Neolithic period and (d) Bronze Age (at the time of the wrecking) in the examined area.

In addition, sea level most probably did not rise gradually but by standstills as is suggested by the existence of a series of scarps on seismic profiles (see chapter 4.2). The link between the increases of the number of submerged shore markers at the time of stadial events could be explained by the findings of worldwide studies which demonstrate rise of the sea level in high rates preceding the stadial event and a slowdown of sea level rise during the establishment of it, regardless if the stadials are occurring within glacial (Yokoyama and Esat, 2011) or interglacial periods (Kendall et al., 2008). Seismic profiling surveys conducted on the shelves of Argolid gulf (van Andel and Lianos, 1984) and Dokos Island (Papatheodorou et al., 2008) also reported the occurrence of submerged features not randomly distributed but cluster at a limited number of water depths. The comparison of the present study findings with those records present coincidence for the cluster depths of scarps at around 100 m, 65 m, 50 m and 46–48 m (Fig. 5c), suggesting an overall sea level stand in the area at least at these depths, regardless if the triggering mechanism was climatic or tectonic.

## 7. Conclusions

The bathymetric, seismic profiling and side scan sonar data sets acquired from the marine surveying of the southwestern Argosaronic gulf helped to reconstruct the evolution of the paleo shoreline since the Paleolithic period. The acoustic data together with sedimentological data and existing information of relative sea level change curves suggests that the sea level rise after the last glaciation resulted to important changes in the extent of the coastal zone. The produced scenarios suggest that the low sea level exposed at least 11 km<sup>2</sup> of coast during the Upper Paleolithic period. At that time Poros and Modi islands were connected to the Peloponnesus. Subsequently, sea level rise during the Mesolithic formed a well-protected bay between Poros Island and Peloponnesus (Monastiriou Bay and disconnected the Modi Islet from Poros Island). The coastal zone reached the present configuration around Late Bronze Age, the time of the ancient shipwreck discovered offshore Modi Islet. The submerged coasts could be potential areas of archaeological interest since the examined area is habited continuously from the Paleolithic period.

Furthermore, the detection and mapping of scarps on the seismic profiles of the present study are in agreement with the findings of previous studies from the broader area and imply that the sea level rise at least from the Last Glacial maximum until the onset of Holocene presented standstills.

At the location of the Late Bronze shipwreck, offshore Modi Islet, the rocky seafloor covered by thin, coarse grained sediments produced unfordable conditions for the preservation of the wreck. Additional, the texture of the seafloor in conjunction with the nature of the wreck (ceramic remains from the cargo scattered in between the rocks) did not allow a reliable mapping of the wreck. However, high resolution acoustic data incorporating echo sounding, seismic profiling and side scan sonar data-sets, established a fundamental data base for the monitoring and future surveying of the site. The comparison of the seismic and side scan records figure eight locations as underwater artifacts and of potential archaeological value.

## Acknowledgments

The authors thank the members of Hellenic Institute for marine Archaeology (H.I.M.A.) for their valuable support during the field work. They would like to thank all reviewers and Guest Editor Matthieu Ghilardi for their helpful comments that contributed to improving the paper. This survey was funded by the “Basic Research Program K. Karatheodori 2011–2014” of the University of Patras (D176).

## References

- Agouridis, C., 1999. Point Iria wreck: discovery and excavation. In: Phelps, W., Lolos, Y., Vichos, Y. (Eds.), *The Point Iria Wreck: Interconnections in the Mediterranean ca.1200 BC*, Proceedings of the International Conference, Island of Spetses, pp. 25–42.
- Agouridis, C., 2011. The Late Bronze Age Shipwreck of the Islet of Modi (Poros). *Skyllis*. pp. 25–34.
- Agouridis, C., 1997. Sea routes and navigation in the third millenium aegean. *Oxf. J. Archaeol.* 16, 1–24.
- Bailey, G.N., 2004. World prehistory from the margins: the role of coastlines in human evolution. *Journal of Interdisciplinary Studies in History and Archaeology* 1, 39–50.
- Bailey, G.N., Flemming, N.C., 2008. Archaeology of the continental shelf: marine resources, submerged landscapes and underwater archaeology. *Quat. Sci. Rev.* 27, 2153–2165. <http://dx.doi.org/10.1016/j.quascirev.2008.08.012>.
- Bass, G.F., 1967. Cape Gelidonya: a bronze age shipwreck. *T. Am. Philos. Soc.* 57 (8) (Philadelphia).
- Chalari, A., Papatheodorou, G., Geraga, M., Christodoulou, D., Ferentinos, G., 2009. A marine geophysical survey illustrates Alexandria's Hellenistic past. *Z. Geomorphol.* 53, 191–212.
- Damuth, J.E., 1975. Echo character of the western equatorial Atlantic floor and its relationships to the dispersal and distribution of terrigenous sediments. *Mar. Geol.* 18, 17–45.
- Dao, P., 2011. Marine Geophysical and Geomorphic Survey of Submerged Bronze Age Shorelines and Anchorage Sites at Kalamianos (Korphos, Greece). McMaster University (Open Access Dissertations and Theses. Paper 6310) <http://hdl.handle.net/11375/11336>.
- European Commission, 2006. Regulation (EC) 1967/2006 of the Council of 21 December 2006 concerning management measures for the sustainable exploitation of fishery resources in the Mediterranean Sea. *Off. J. Eur. Union* 50, L36/6–L36/30.
- Ferentinos, G., Gkioni, M., Geraga, M., Papatheodorou, G., 2012. Early seafaring activity in the southern Ionian Islands, Mediterranean Sea. *J. Archaeol. Sci.* 39, 2167–2176. <http://dx.doi.org/10.1016/j.jas.2012.01.032>.
- Ferentinos, G., Papatheodorou, G., Geraga, M., Christodoulou, D., Fakiris, E., Iatrou, M., 2015. The disappearance of helike-classical Greece-New remote sensing and geologic evidence. *Remote Sens.* 7, 1263–1278. <http://dx.doi.org/10.3390/rs70201263>.
- Flemming, N.C., Czartoryska, N.M.G., Hunter, P.M., 1971. Archaeological evidence for eustatic and tectonic components of relative sea level change in the south Aegean. In: Blackman, D.J. (Ed.), *Marine Archaeology. Proceedings of the 23th Symposium of the Colston Research Society*, University of Bristol, pp. 1–63.
- Flemming, N.C., 1978. Holocene eustatic changes and coastal tectonics in the northeast Mediterranean: implications for models of crustal consumption. *Philos. Trans. R. Soc. A Math. Phys. Eng. Sci.* 289, 405–458. <http://dx.doi.org/10.1098/rsta.1978.0065>.
- Folk, R.L., 1974. *Petrology of Sedimentary Rocks*. Hemphil Publishing Company, Austin, Texas 0-914696-14-9.
- Fytikas, M., Innocenti, F., Kolios, N., Manetti, P., Mazzuoli, R., 1986. The Plio-quaternary volcanism of Saronikos area (western part of the Aegean volcanic arc). *Ann. Géol. Pays Hellén.* 33, 23–45.
- Galili, E., Gale, N., Rosen, B., 2013. A late bronze age shipwreck with a metal cargo from Hishuley Carmel. *Israel. Int. J. Naut. Archaeol.* 42 (1), 2–23.
- Galili, E., Sharvit, J., 1999. Haifa, Underwater Surveys, *Hadashot Arkheologiyot* 110. Excavations and Surveys. pp. 15–20.
- Georgiadis, M., Papatheodorou, G., Tzanatos, E., Geraga, M., Ramfos, A., Koutsikopoulos, C., Ferentinos, G., 2009. Coralligène formations in the eastern Mediterranean Sea: morphology, distribution, mapping and relation to fisheries in the southern Aegean Sea (Greece) based on high-resolution acoustics. *J. Exp. Mar. Biol. Ecol.* 368, 44–58. <http://dx.doi.org/10.1016/j.jembe.2008.10.001>.
- Geraga, M., Papatheodorou, G., Ferentinos, G., Fakiris, E., Christodoulou, D., Georgiou, N., Dimas, X., Iatrou, M., Kordella, S., Sotiropoulos, G., Mentogiannis, V., Delaporta, K., 2015. The study of an ancient shipwreck using remote sensing techniques, in Kefalonia Isl (Ionian Sea). *Archaeologia Maritima Mediterranea.* 12, pp. 181–198.
- Geraga, M., Ioakim, C., Lykousis, V., Tsaila-monopolis, S., Mylona, G., 2010. The high-resolution palaeoclimatic and palaeoceanographic history of the last 24,000 years in the central Aegean Sea, Greece. *Palaeogeogr. Palaeoclimatol. Palaeoecol.* 287, 101–115. <http://dx.doi.org/10.1016/j.palaeo.2010.01.023>.
- Geraga, M., Tsaila-monopolis, S., Ioakim, C., Papatheodorou, G., Ferentinos, G., 2000. Evaluation of Palaeoenvironmental Changes During the Last 18,000 Years in the Myrtoon Basin, SW Aegean Sea. 156 pp. 1–17.
- Gregory, D., 2006. Mapping navigational hazards as areas of maritime archaeological potential: the effects of sediment type on the preservation of archaeological materials. Report From the Department of Conservation National Museum of Denmark, pp. 1–17. <http://archaeologydataservice.ac.uk>.
- Henderson, J., Pizarro, O., Johnson-Roberson, M., Mahon, I., 2013. Mapping submerged archaeological sites using stereo-vision photogrammetry. *Int. J. Naut. Archaeol.* 42, 243–256. <http://dx.doi.org/10.1111/1095-9270.12016>.
- Kendall, R.A., Mitrovica, J.X., Milne, G.A., Törnqvist, T.E., Li, Y., 2008. The sea-level fingerprint of the 8.2 ka climate event. *Geology* 36, 423–426. <http://dx.doi.org/10.1130/G24550A.1>.
- Kiparissis, S., Fakiris, E., Papatheodorou, G., Geraga, M., Kornaros, M., Kapareliotis, A., Ferentinos, G., 2011. Illegal trawling and induced invasive algal spread as collaborative factors in a *Posidonia oceanica* meadow degradation. *Biol. Invasions* 13, 669–678. <http://dx.doi.org/10.1007/s10530-010-9858-9>.
- Kolaiti, E., Mourtzas, N.D., 2016. Upper Holocene sea level changes in the west Saronic gulf, Greece. *Quat. Int.* 401, 71–90. <http://dx.doi.org/10.1016/j.quaint.2015.06.024>.
- Konsolaki-Giannopoulou, H., 2009. The new findings from Troizinia. From Mesogia to Argosaronikos, 2nd Ephorate of Prehistoric and Classical Antiquities. ISBN: 978-960-85371-7-0, pp. 497–518.

- Koukousioura, O., Dimiza, M.D., Triantaphyllou, M.V., Hallock, P., 2011. Living benthic foraminifera as an environmental proxy in coastal ecosystems: a case study from the Aegean Sea (Greece, NE Mediterranean). *J. Mar. Syst.* 88, 489–501. <http://dx.doi.org/10.1016/j.jmarsys.2011.06.004>.
- Lambeck, K., 1995. Late Pleistocene and Holocene sea-level change in Greece and south-western Turkey: a separation of eustatic, isostatic and tectonic contributions. *Geophys. J. Int.* 122, 1022–1044. <http://dx.doi.org/10.1111/j.1365-246X.1995.tb06853.x>.
- Lambeck, K., 1996. Sea-level change and shore-line evolution in Aegean Greece since upper Palaeolithic time. *Antiquity* 70, 588–611. <http://dx.doi.org/10.1017/S0003598X00083733>.
- Lambeck, K., Esat, T.M., Potter, E.-K., 2002. Links between climate and sea levels for the past three million years. *Nature* 419, 199–206. <http://dx.doi.org/10.1038/nature01089>.
- Lambeck, K., Purcell, A., 2005. Sea-level change in the Mediterranean Sea since the LGM: model predictions for tectonically stable areas. *Quat. Sci. Rev.* 24, 1969–1988. <http://dx.doi.org/10.1016/j.quascirev.2004.06.025>.
- Loeblich, A.R., Tappan, H., 1987. *Foraminiferal Genera and Their Classification*. 2. Springer Science-Business Media, LLC 978-1-4899-5762-7.
- Lolos, Y., 1999. The cargo of pottery from the Point Iria wreck: character and implications. In: Phelps, W., Lolos, Y., Vichos, Y. (Eds.), *The Point Iria Wreck: Interconnections in the Mediterranean ca.1200 BC*, Proceedings of the International Conference, Island of Spetses, pp. 43–53.
- Naehser, S., Geraga, M., Papatheodorou, G., Ferentinos, G., Kaberi, H., Schubert, C.J., Dynamics, P., 2012. Environmental Variations In A Semi-Enclosed Embayment (Amvrakikos Gulf, Greece) – Reconstructions Based on Benthic Foraminifera Abundance and Lipid Biomarker Pattern. pp. 5081–5094 <http://dx.doi.org/10.5194/bg-9-5081-2012>.
- Nixon, F.C., Reinhardt, E.G., Rothaus, R., 2009. Foraminifera and tidal notches: dating neotectonic events at Korphos, Greece. *Mar. Geol.* 257, 41–53. <http://dx.doi.org/10.1016/j.margeo.2008.10.011>.
- Noble, P.J., Ball, G.J., Zimmerman, S.H., Maloney, J., Smith, S.B., Kent, G., Adams, K.D., Karlin, R.E., Driscoll, N., 2016. Holocene paleoclimate history of Fallen Leaf Lake, CA, from geochemistry and sedimentology of well-dated sediment cores. *Quat. Sci. Rev.* 131, 193–210. <http://dx.doi.org/10.1016/j.quascirev.2015.10.037>.
- Papathanasopoulos, G., Vichos, Y., Lolos, Y., Tsouhlos, N., Antonopoulos, F., Kritzas, H., other members of H.I.M.A., 1989–1992. *The Project of Dokos. Enalia I-V, H.I.M.A., Athens*.
- Papatheodorou, G., Geraga, M., Ferentinos, G., 2005. The Navarino naval battle site, Greece – an integrated remote sensing survey and a rational management approach. *Int. J. Naut. Archaeol.* 34 (1), 95–109. <http://dx.doi.org/10.1111/j.1095-9270.2005.00047.x>.
- Papatheodorou, G., Geraga, M., Ferentinos, G., 2008. In: Facorellis, Y., Zacharias, N., Polkkreti, K. (Eds.), *The Study of Coastal Palaeogeography of Dokos Island, Greece, Using Remote Sensing Techniques*. *Brit. Archaeol. Rep. In.* 1746. ISBN: 978 1 4073 01884, pp. 65–71.
- Pausanias, Description of Greece, 1961. An English Translation by Jones, W.H.S., Ormerod, H.A., Wycherley, R.E., (4 Volumes), Harvard University Press.
- Pavlopoulos, K., Kapsimalis, V., Theodorakopoulou, K., Panagiotopoulos, I.P., 2012. Vertical displacement trends in the Aegean coastal zone (NE Mediterranean) during the Holocene assessed by geo-archaeological data. *The Holocene* 22, 717–728. <http://dx.doi.org/10.1177/0959683611423683>.
- Perles, C., 1987a. Les industries lithiques Taillées de Franchthi. In: Jacobsen, T.W. (Ed.), Tome I. Présentation générale et Industries Paléolithiques, Excavations at Franchthi Cave, Greece. Indiana University Press, Bloomington and Indianapolis (fasc. 5).
- Perles, C., 1987b. Les industries lithiques Taillées de Franchthi (Argolide, Grèce). In: Jacobsen, T.W. (Ed.), Tome II. Les Industries du Mésolithique et du Néolithique initial, Excavations at Franchthi Cave, Greece. Indiana University Press, Bloomington and Indianapolis (fasc.5).
- Pulak, C., 1998. The Uluburun shipwreck: an overview. *Int. J. Naut. Archaeol.* 27 (3), 188–224.
- Quinn, R., Boland, D., 2010. The role of time-lapse bathymetric surveys in assessing morphological change at shipwreck sites. *J. Archaeol. Sci.* 37, 2938–2946. <http://dx.doi.org/10.1016/j.jas.2010.07.005>.
- Quinn, R., Forsythe, W., Breen, C., Boland, D., Lane, P., Omar, A.L., 2007. Process-based models for port evolution and wreck site formation at Mombasa, Kenya. *J. Archaeol. Sci.* 34, 1449–1460. <http://dx.doi.org/10.1016/j.jas.2006.11.003>.
- Runnels, C.N., van Andel, T.H., 1987. The evolution of settlement in the southern Argolid, Greece: an economic explanation. *Hesperia* 56 (3), 303–334. <http://dx.doi.org/10.2307/148096>.
- Sakellariou, D., Georgiou, P., Mallios, A., Kapsimalis, V., Kourkoumelis, D., Micha, P., Theodoulou, T., Dellaporta, K., 2007. Searching for ancient shipwrecks in the aegean sea: the discovery of chios and kythnos hellenistic wrecks with the use of marine geological-geophysical methods. *Int. J. Naut. Archaeol.* 36, 365–381. <http://dx.doi.org/10.1111/j.1095-9270.2006.00133.x>.
- Sanchez-Cabeza, J.A., Masque, P., Ani-Ragolta, I., 1998. Lead-210 and polonium-210 analysis in sediments and soils by microwave acid digestion. *J. Radioanal. Nucl. Chem.* 227, 19–22. <http://dx.doi.org/10.1007/BF02386425>.
- SASMAP, Development of Tools and Techniques to Survey, Assess, Stabilise, Monitor and Preserve Underwater Archaeological Sites. <http://sasmap.eu> (accessed 15.6.16).
- Schwandner, F.M., 1998. Polyphase Meso-to Cenozoic structural development on Poros island (Greece). *Bulletin of the Geological Society of Greece. Proceedings of the 8th International Congress, XXXII/1*, pp. 129–136.
- SPLASCOS, Submerged Prehistoric Archaeology and Landscapes of the Continental Shelf. <http://www.splashcos.org> (accessed 15.6.16).
- Tartaron, T.F., Pullen, D.J., Dunn, R.K., Tzortzopoulou-Gregory, L., Dill, A., Boyce, J.I., 2011. The Saronic Harbors Archaeological Research Project (SHARP): investigations at Mycenaean Kalamianos, 2007–2009. *Hesperia* 80 (4), 559–634.
- Van Andel, T.H., Lianos, N., 1984. High resolution seismic reflection profiles for the reconstruction of post-glacial transgressive shorelines: an example from Greece. *Quat. Res.* 22, 31–45.
- Wachsmann, S., 2011. Deep-submergence archaeology. In: Catsambis, A., Ford, B., Hamilton, D. (Eds.), *The Oxford Handbook of Marine Archaeology*. Oxford University Press, New York, pp. 202–231.
- Westley, K., Quinn, R., Forsythe, W., Plets, R., Bell, T., Benetti, S., McGrath, F., Robinson, R., 2011. Mapping submerged landscapes using multibeam bathymetric data: a case study from the north coast of Ireland. *Int. J. Naut. Archaeol.* 40 (1), 99–112. <http://dx.doi.org/10.1111/j.1095-9270.2010.00272.x> (2010).
- Wheeler, A.J., 2002. Environmental controls on shipwreck preservation: the Irish context. *J. Archaeol. Sci.* 29, 1149–1159. <http://dx.doi.org/10.1006/jasc.2001.0762>.
- Yokoyama, Y., Esat, Y., 2011. Global climate and sea level: enduring variability and rapid fluctuations over the past 150,000 years. *Oceanography* 24, 54–69. <http://dx.doi.org/10.5670/oceanog.2011.27.COPYRIGHT>.